

On Filamentations and Virtual Knots

David Hrencecin

Department of Mathematics, Statistics
and Computer Science (m/c 249)
851 South Morgan Street
University of Illinois at Chicago
Chicago, Illinois 60607-7045
<dhren@math.uic.edu>

and

Louis H. Kauffman

Department of Mathematics, Statistics
and Computer Science (m/c 249)
851 South Morgan Street
University of Illinois at Chicago
Chicago, Illinois 60607-7045
<kauffman@uic.edu>

1 Introduction

Virtual knot theory is a recent generalization of knot theory. One motivation for studying virtual knots comes from the methods of describing knots through the use of chord diagrams. In Section 2 we give the basic definitions for this point of view. In particular, we define oriented chord diagrams and arrow diagrams. The definition for a virtual knot is also given, though we recommend [13] as an introduction for the reader who is not already familiar with virtual knot theory. Flat virtual diagrams and their equivalence classes are introduced in Section 3.

In Section 4, we define a filamentation on a Gauss chord diagram. Filamentations were first introduced by Scott Carter as a tool for detecting when an immersed curve can be bounded by a disk. We show that they can also detect when virtual knots are non-trivial. We demonstrate that a virtual knot diagram cannot be reduced to a classical knot whenever a filamentation does not exist on its chord diagram. This result is Theorem 4.10, which we prove from our combinatorial point of view. In fact, we prove that whenever there is no filamentation on a chord diagram, then any associated flat virtual diagram cannot be reduced to a classical diagram. There are many open problems in the

classification of flat virtual knots.

One interesting result of Theorem 4.10 is that we have found an infinite class of chord diagrams for which no filamentation exists. Section 5 explores this infinite class of virtual knots (K_n) related to the chord diagrams. The generalizations of both the Jones polynomial and the fundamental group to virtual knots cannot detect any of these K_n . Using filamentations, we are able to show that each K_n is non-trivial, although this method cannot distinguish between the K_n . In Section 6, we prove that the K_n are an infinite class of mutually distinct knots.

We would like to thank Scott Carter, Heather Dye and David Radford for their very helpful conversations in the course of preparing this paper.

2 Definitions

We define a knot K in the combinatorial sense, as a class of diagrams which represent a generic projection of an embedding $S^1 \rightarrow S^3$ or $S^1 \sqcup \dots \sqcup S^1 \rightarrow S^3$. Each circle represented in such a diagram is called a component, and if there is more than one component, the diagram (or related class) is sometimes referred to as a link. A strand in a knot diagram is the projection of a connected interval in the embedded curve. In a knot diagram, certain arcs of the projection of the curve embedded in space are eliminated to form a knot diagram, creating broken strands that indicate the over and under crossings. At each crossing in the diagram there is an indicated over strand and a broken under strand. In this sense, there are two local strands at any crossing in a diagram. Any time we refer to a strand of a crossing, we mean one of these two local strands.

Definition 2.1. Two knot diagrams K and K' are said to be *equivalent* when there is a finite sequence of the following (Reidemeister) moves which transform K into K' :

$$\begin{array}{ccc}
 \text{(R1)} & \begin{array}{c} \text{Diagram of a loop with a crossing} \\ \rightleftharpoons \\ \text{Diagram of a simple strand} \end{array} & \text{(R2)} & \begin{array}{c} \text{Diagram of two strands crossing} \\ \rightleftharpoons \\ \text{Diagram of two strands crossing} \end{array} \\
 & & \text{(R3)} & \begin{array}{c} \text{Diagram of a crossing with over/under strands} \\ \rightleftharpoons \\ \text{Diagram of a crossing with over/under strands} \end{array}
 \end{array}$$

A *knot* is an equivalence class of knot diagrams under the Reidemeister moves.

A knot can have an orientation. This is indicated on a knot diagram by drawing an arrowhead on one or more strands in such a way that each component has a consistent labelling. The Reidemeister moves for an oriented knot are the same as for unoriented knots. We are free to apply the moves without paying attention to the particular orientations of the strands involved.

There is also the notion of more than one kind of Reidemeister equivalence. *Regular isotopy* is equivalence under only the R2 and R3 moves. *Ambient isotopy*

is equivalence under all three moves. It is useful to distinguish between the two because there are invariants which only cover regular isotopy. For a more general treatise on knot theory, see [12] and [16].

In the study of Vassiliev (or finite type) knot invariants, chord diagrams and weight systems have been used as a calculational tool [1, 8, 19]. We will examine chord diagrams further and investigate their usefulness in the general theory of knots. Briefly, a chord diagram is a circle (or set of disjoint circles¹) with pairs of points on it, where each pair of points is connected by a line segment, or *chord*, in the interior of the circle. We will assume the convention that the circle in a chord diagram is oriented in a counterclockwise direction. One way of thinking of a chord diagram is to view the outer circle(s) as the pre-image of the projection of a knot.

Definition 2.2. The *universe* (or shadow) [13] of a knot is a generic projection of the embedding without specified over or under crossings. We sometimes refer to this as a flattened knot diagram.

The circle(s) in a chord diagram can be interpreted as the domain of a knot projection. Each circle corresponds to a component in an associated embedding. Hence we will sometimes refer to each circle as a component of the chord diagram. Each chord connects the double points corresponding to a particular crossing. This does not encode the types of crossings involved. Additional structure is needed in order to describe a knot diagram completely.

One solution to the problem of encoding the knot diagram is to add a sign and a direction to each chord [8, 18, 19].

Definition 2.3. A *signed arrow diagram* is a chord diagram in which each chord is decorated with an arrow and given a sign. The sign determines the crossing orientation and the arrow points to the chord endpoint which lies on the undercrossing strand in a related knot diagram.

Definition 2.4. Dropping the arrow directions from a signed arrow diagram leaves a chord diagram with a single sign on each chord. We call this a *signed chord diagram*.

There is a slight problem with developing a theory using signed arrow diagrams. We would like to have a chord diagram analogue to oriented knot universes which generalizes signed arrow diagrams. However in this case, the arrow and sign information are mostly interdependent. Signed chord diagrams do not store the same kind of information that universes do. It turns out that the Jones polynomial depends solely on the underlying signed chord diagram of a knot, and this certainly cannot be said for knot universes. Each universe covers multiple knot classes, many of which have different Jones polynomials.

¹For links, we use a circle to represent each component. Each crossing involving a single component is represented by a chord contained in the interior of that component's circle. All crossings between two different components are represented by chords between each circles' exterior.

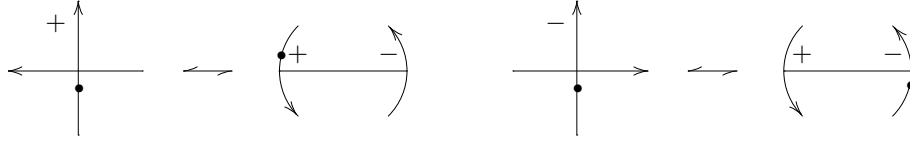


Figure 1: Crossing conventions for oriented chord diagrams

Our enhancements will modify signed arrow diagrams in a way that allows us to generalize to oriented knot universes. We start by defining an *oriented chord diagram* and then give a new definition of an *arrow diagram* which builds on the underlying structure of an oriented chord diagram.

2.1 Oriented Chord Diagrams

Definition 2.5. An *oriented chord diagram*, or OCD, is a chord diagram with a labelling of ‘+’ or ‘-’ on each chord endpoint, so that each chord connects points of opposite sign.

An OCD encodes the universe of a knot diagram. A neighborhood of a chord endpoint (restricted to the circle) corresponds to one strand of a crossing in a universe, and the sign on each chord endpoint determines the local orientation relative to that strand. In order to label a chord endpoint, start with its corresponding strand in the universe and view that strand in the direction induced by the counter-clockwise orientation of the circle. Now look at the other strand of the crossing. If it passes from right to left, label the current chord endpoint with a ‘+’. Otherwise label it ‘-’. (See Figure 1). In other words, we view the two strands as vectors in the plane of projection. The orientation comes from a standard right handed convention relating the first vector to the second. Switching the point of view from one chord endpoint to the other reverses the local orientation.

Suppose we wish to recapture the universe from a single component OCD. Choose a point on the circle that is not a chord endpoint. Starting at this point, follow around the circle in a counterclockwise direction. While traversing the circle, draw a curve forming a diagram as follows:

- Each time the first endpoint of a new chord is encountered, draw a crossing obeying the sign convention and continue along the curve.
- Whenever possible, draw the curve so that the only crossings which occur correspond to chords in the diagram.
- When the second endpoint of a chord is encountered, connect the curve through the previously drawn crossing in the direction indicated by the sign.
- Connect the endpoints of the curve when all the chords are accounted for.

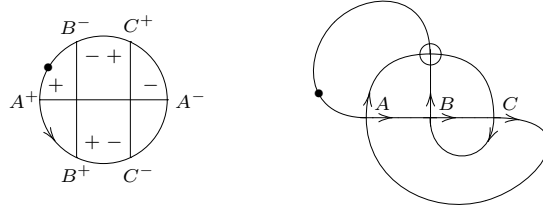


Figure 2: An oriented chord diagram and related knot universe

- If the curve is forced to cross itself at any point, circle the forced crossings to distinguish them from those associated with chords.

Figure 2 shows a knot universe along with the OCD which represents it. If there are multiple components in the OCD, proceed in the same fashion for each one.

In the resulting universe, any crossing indicated by a chord in the OCD is called a real (or classical) crossing. The remaining crossings – those forced by the planar configuration of real crossings – are called virtual. Virtual crossings are like edge crossings in a drawing of a non-planar graph; they do not exist in the original chord diagram, but are artifacts of drawing the associated planar universe.

Definition 2.6. When we refer to crossing *type*, we mean the distinction between real and virtual.

In addition to diagrammatic representation, an OCD can be encoded in terms of the chord endpoints and how they are ordered while traversing the circle(s). Suppose \mathcal{D} is an OCD with n chords, $\{x_1, x_2, \dots, x_n\}$. For each chord x_i , label the positive endpoint X_i^+ and the negative² endpoint X_i^- . In this paper, we will stick to the convention of using lowercase letters when referring to chords and the corresponding uppercase letters when referring to endpoints. If c is a chord in \mathcal{D} , then C^+ and C^- are the positively and negatively (resp.) oriented endpoints of c .

To encode an oriented chord diagram \mathcal{D} , begin at any nonsingular point on the circle. Traverse the circle \mathcal{D} in a counterclockwise direction and write down the appropriate label for each endpoint as you pass it, until you return to your original point on the circle. Multiple components generate multiple codes: one for each component. Consider the OCD in Figure 2. An example of a code associated with it is $A^+B^+C^-A^-C^+B^-$. These codes are unique up to cyclic permutation (to account for where you start on the circle), along with any permutation of the chord labels.

That is,

$$A^+B^+C^-A^-C^+B^-, \quad C^-A^-C^+B^-A^+B^+, \quad \text{and} \quad A^+C^+B^-A^-B^+C^-$$

are all codes for the same OCD.

²We also use the negative superscript as an orientation reversing operator: $(A^-)^- = A^+$.

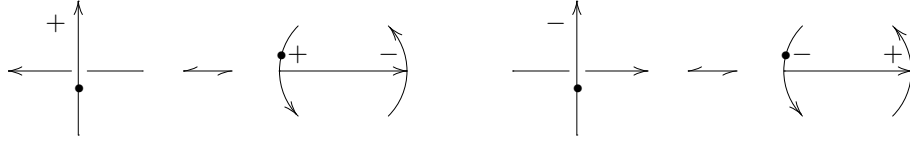


Figure 3: Crossing conventions for arrow diagrams

2.2 Arrow Diagrams

So far, we have described OCD's and their relationship with knot universes. We define an arrow diagram within this framework.

Definition 2.7. An *arrow diagram*, or AD, is an oriented chord diagram in which the chords are replaced with arrows. The direction of each arrow gives the extra structure on a crossing in the related knot universe by the convention that the arrow points from the overcrossing to the undercrossing strand.

Note that the local orientation on the base endpoint of an arrow (corresponding to the overcrossing strand) matches the classical knot theoretical convention of crossing sign for an oriented knot (see Figure 3). The local orientation of one chord endpoint is always opposite to the other endpoint, so we will only label the base endpoint of each arrow in an AD. On the surface, an arrow diagram looks just like a signed arrow diagram. The difference is that the arrow diagram sign refers specifically to the local orientation of the arrow basepoint, rather than the sign of the arrow itself.

For the purposes of this paper, the code associated with an arrow diagram will be the same as the code associated with the underlying OCD. If more information is needed, we can use the subscripts 'o' and 'u' to denote arrow basepoints and endpoints (respectively). For example, $A_o^+ B_u^+ C_u^- A_u^- C_o^+ B_o^-$ encodes an arrow diagram with the same underlying code as the OCD in Figure 2. We emphasize again that this is not the same as the convention for signed arrow diagrams where only one sign is associated with each arrow.

We can take the set of all arrow diagrams and define an equivalence relation under the Reidemeister moves translated into AD form (See [8]). Figure 4 lists these moves. The ϵ on the arrows is meant to be either $+$ or $-$. Each arc represents a portion of a circle in an arrow diagram, but it is not necessary to assume that the relative arc placements must be as shown. In the AD_2 move, the two arcs might lie on separate circles of a multiple component AD. Further, in the AD_3 move, we allow flexibility in the ordering of the arcs, even within a single component diagram. Simply put, the arc placements in a single application of an AD move can differ from Figure 4, provided that arc ordering does not change across the move.

Consider the lower left version of the AD_3 move. One application of AD_3

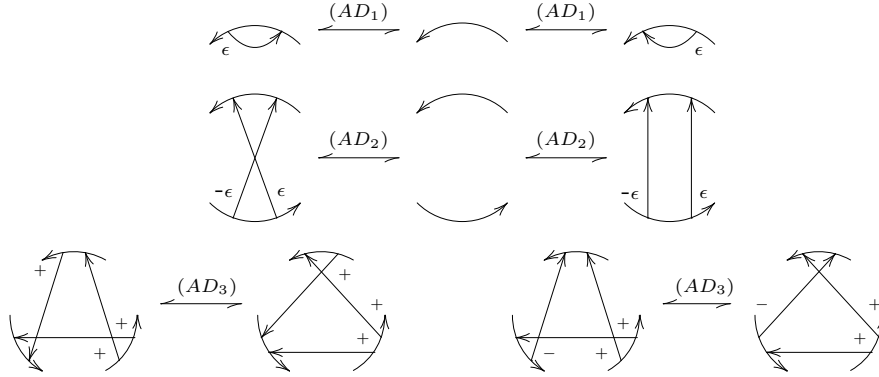


Figure 4: The arrow diagram moves

might change an associated code's subcode from

$$A_u^- B_u^- \dots C_o^+ A_o^+ \dots C_u^- B_o^+ \quad \text{to} \quad B_u^- A_u^- \dots A_o^+ C_o^+ \dots B_o^+ C_u^-$$

under the move. Another example of AD_3 might change the subcode from

$$C_o^+ A_o^+ \dots A_u^- B_u^- \dots C_u^- B_o^+ \quad \text{to} \quad A_o^+ C_o^+ \dots B_u^- A_u^- \dots B_o^+ C_u^-$$

in an arrow diagram. With this in mind, these moves completely describe the reformulation of Reidemeister moves into diagrammatic form and translate the combinatorics of knot equivalence into arrow equivalence.

3 Virtual Knots

It turns out that this new class of objects generalizes the classical knots. Given an abstract arrow diagram \mathcal{A} , we find that it is not always possible to realize \mathcal{A} as a knot projection on a sphere or plane. Such a non-planar AD is a virtual knot. A more diagrammatic definition follows:

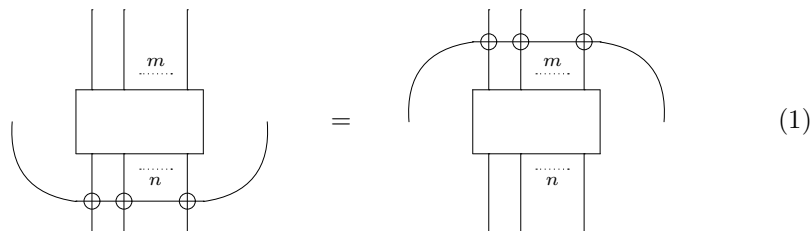
Definition 3.1. A *virtual knot diagram* is a generic immersion $S^1 \sqcup \dots \sqcup S^1 \rightarrow \mathbb{R}^2$ such that each double point is labelled with either a real (over or under) or a virtual (circled) crossing. Thus a *virtual knot* is a class of equivalent virtual diagrams, where two virtual knot diagrams are said to be equivalent when one can be transformed into the other by a finite sequence of real Reidemeister moves (R1), (R2) and (R3), along with the following virtual moves:





As in the classical case, a virtual knot with multiple components is sometimes called a virtual link. For this paper, we will use the term ‘virtual knot’ to refer to both virtual knots and links. When we do not wish to consider virtual crossings, we will use the term ‘classical knot’ to mean knots and links without virtual crossings.

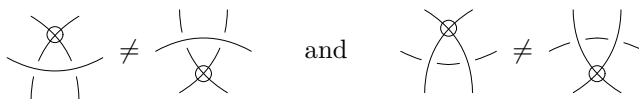
An alternate definition to virtual Reidemeister equivalence is to allow the classical Reidemeister moves with the addition of a more general “detour move” (See [13, 14]):



In the detour move, any number of strands may emanate from the top and bottom of the tangle (represented by a box). The idea is that in a virtual diagram, if we have an arc with any number of consecutive virtual crossings, then we can cut that arc out and replace it with another arc connecting the same points, provided that any crossings on the new arc are also virtual. It is easily seen that this yields the same equivalence.

Definition 3.2. If K is a knot diagram, then $AD(K)$ is the arrow diagram related to K .

Notice that there are some mixed moves which are not allowed. Consider the following moves:



These are forbidden as knot diagrammatical analogues to the AD moves. They change the related arrow diagram in a manner which is not equivalent under the AD moves; they permute two adjacent arrow endpoints. However, inclusion of the above left (overstrand) version of this move has been studied in the form of welded braids [5, 7], a generalization of braid theory preceding virtual knot theory.

From the definition, we note that a virtual knot or link can also be classical. This happens when it can be represented by a diagram in which all of the crossings are real. Further, since the virtual moves (V1)-(V4) leave the related arrow diagram unchanged, they also preserve the classical knot type. However,

it is possible to apply an arrow diagram move to a chord diagram for a classical knot in such a way that the resulting knot diagram is no longer classical.

There has been progress in applying well known knot invariants to the virtual theory. In [13] Kauffman extended the fundamental group, the Jones polynomial and classes of quantum link invariants to virtual knots and gave examples of non-trivial virtual knots with trivial Jones Polynomial and trivial³ fundamental group. We will cover the fundamental group and the Jones polynomial in Section 5.

One of the results we will assume is the following, proved by Kauffman along with Goussarov, Polyak and Viro:

Lemma 3.3. *If K and K' are classical knots which are equivalent under virtual Reidemeister equivalence, then they are also equivalent under classical Reidemeister equivalence.*

We will also use the following result:

Theorem 3.4. *Virtual equivalence and AD equivalence are the same thing. That is, if two arrow diagrams are equivalent under AD moves, then any virtual knots related to those two diagrams will be virtually equivalent. Likewise, if $K \simeq K'$, then $AD(K) \simeq AD(K')$.*

Proof. This is a direct result of the definitions. ■

An immediate question that arises is how to determine when a virtual knot is classical. In [13], Kauffman introduces flat Reidemeister equivalence as one approach to this problem.

Definition 3.5. A *flat Reidemeister move* is a classical or virtual Reidemeister move in which the over/under information at each real crossing is suppressed, so that all that is important is the distinction between crossing types (real and virtual). Two universes are *flat (Reidemeister) equivalent* if there is a finite sequence of flat Reidemeister moves taking the one universe to the other. An equivalence class of knot universes under flat equivalence is called a *flat knot*.

In Figure 5, we illustrate the (flat) Reidemeister moves for flat virtual diagrams. Note that a sequence of virtual crossings can be detoured across flat crossings (using the mixed move given by IV), but not vice versa. The virtual detour move given in (1) applies for flat knots as well, and can be thought of as equivalent to move IV in the presence of the other moves.

The remarkable fact about flat virtual diagrams is that while they are often non-trivial (and hence non-classical), we have very few invariants at the present time which detect and classify them. For example, consider the following flat diagram:

³by trivial fundamental group, we mean a group isomorphic to the integers

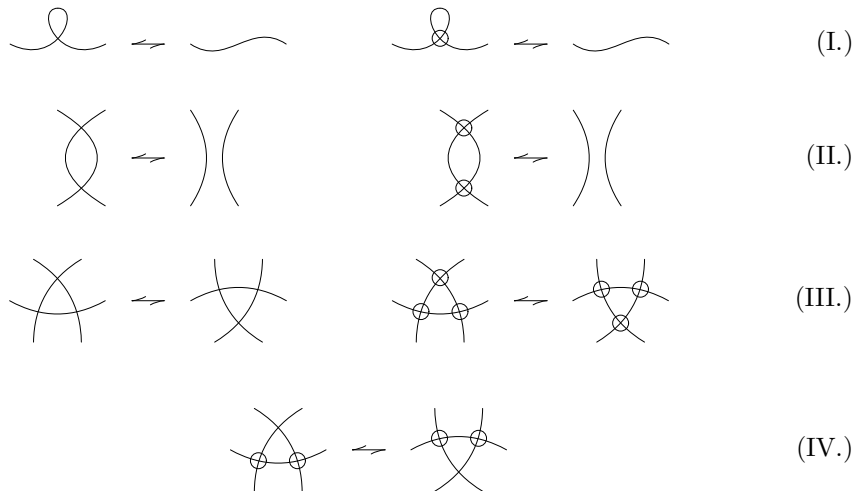
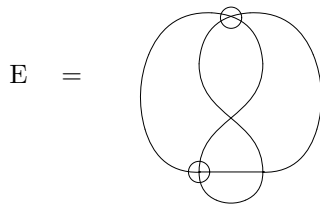
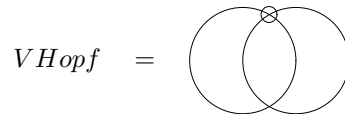


Figure 5: The Flat Reidemeister Moves



At the time of this writing, we do not have a proof that the flat diagram E given above is inequivalent to a circle.

A simple example of a non-trivial flat virtual link is the positive virtual Hopf link, $VHopf$:



Definition 3.6. The *parity* of a link is the parity of the total number of crossings between distinct components. The parity is an invariant of flat virtual links, because it is preserved under the flat Reidemeister moves.

For the virtual Hopf link, the parity is odd and hence $VHopf$ is non-trivial.

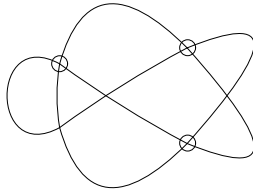
Theorem 3.7. *If a virtual knot is classical, then its related universe is flat equivalent to the unknot.*

Proof. It is well known that every classical knot diagram can be unknotted by choosing and switching a certain number of crossings. The original knot along with this unknotted diagram both share the same universe. As a result, we can always find a sequence of flat moves taking a classical universe to the unknot diagram. ■

Note that a flat virtual diagram is the same as a knot universe, with the additional property that it may also have virtual crossings. For any oriented flat virtual diagram, there is an OCD associated with it in the same way that a chord diagram is associated with an oriented universe. Recall that the chords in an OCD have no arrows and are labelled with signs at their ends corresponding to the crossing orientations of their corresponding curves. Each flat Reidemeister move induces a related OCD move. These OCD moves are the same as the arrow diagram moves in Figure 4 with the arrow endpoints removed⁴. This OCD approach will become useful in the discussion of filamentation invariance.

4 Filamentations on Chord Diagrams

The notion of a filamentation⁵ was first introduced in the early 1990's by Scott Carter in [2, 3, 4] while looking at generic immersions of disks in 3 space. In the particular case where the boundary of the disk is mapped to the boundary of the manifold, he noted that the intersection curves would necessarily have a total net intersection of zero. In 2000, he suggested (private communication) that filamentations could be used to answer a conjecture of Kauffman's in [13] that the following flat knot was non-trivial under flat virtual equivalence:



A knot diagram with the above universe was the first example of a non-trivial virtual knot with trivial Jones polynomial and trivial fundamental group.

Roughly speaking, a filamentation can describe the intersection curves on an immersed disk, much in the same way that a chord diagram describes the double points in an immersed circle. Consider an immersed disk which bounds a flat knot diagram. Wherever the diagram has a flat crossing, the immersed disk will have intersection curves emanating from the crossing. These intersection curves will begin and end at crossings. A filament is a curve from the pre-image of such an intersection curve. Thus, a filament begins at one chord endpoint and ends at another (not necessarily the same) chord endpoint.

⁴To get an oriented chord back from an arrow, we drop the arrow tip and place a sign on that endpoint that is opposite to the one on the basepoint.

⁵also known as bifilarations

Our method will generalize this description so that there is no dependence on immersed curves in space. We describe filamentations in the purely combinatorial context of flat virtual knots so that the existence of a filamentation can be used to determine when a flat knot is non-trivial.

For the remainder of the paper, when we say chord diagram, we are referring generally to OCD's and AD's.

Definition 4.1. A *pairing* \mathcal{P} on a chord diagram \mathcal{D} is a collection of chord pairs such that each chord in \mathcal{D} occurs in exactly one pair in the collection. A chord is allowed to be paired with itself.

For example, the OCD in Figure 2 has the following possible pairings:

$$\begin{aligned} &\{(a, a), (b, c)\} \\ &\{(b, b), (a, c)\} \\ &\{(c, c), (a, b)\} \\ &\{(a, a), (b, b), (c, c)\} \end{aligned} \tag{2}$$

Definition 4.2. A *filament* α associated with a chord pair (x, y) is a generic curve between an endpoint X^ϵ of x and the corresponding endpoint $Y^{-\epsilon}$ of y (where $\epsilon \in \{+, -\}$). Between endpoints, the curve must lie completely in the interior region of one of the circles in \mathcal{D} and may contain a finite number of transverse self-intersections. We orient the filament from the negative endpoint to the positive one.

In general, there are an infinite number of filaments associated with a given pair. For this paper, we will treat a filament associated with a pair as a single class, taken up to planar isotopy of immersed curves with fixed endpoints.

Definition 4.3. The *dual* of a filament $\alpha : X^- \rightarrow Y^+$, denoted α' , is a filament $\alpha' : Y^- \rightarrow X^+$ between the two corresponding chord endpoints Y^- and X^+ of opposite sign.

Definition 4.4. If x and y are distinct chords, then the two filaments associated with the pair (x, y) , namely $\alpha : Y^- \rightarrow X^+$ and its dual $\alpha' : X^- \rightarrow Y^+$, are called *bifilaments*.

Definition 4.5. A *monofilament* is a filament $\alpha : X^- \rightarrow X^+$ associated with a symmetric pair (x, x) . In this case, $\alpha = \alpha'$.

We will refer to distinct pairs (x, y) as bifilament pairs and self-pairs (x, x) as monofilament pairs.

Definition 4.6. When two distinct filaments α and β intersect transversally, they have an *oriented intersection number* $\alpha \overrightarrow{\cap} \beta$. It is calculated by looking at the local orientation (using a right-handed convention) of the crossings between each filament: looking in the direction of α , if β is directed from right to left (left to right), then $\alpha \overrightarrow{\cap} \beta = +1$ ($= -1$). If there are no intersections $\alpha \overrightarrow{\cap} \beta = 0$.

Note that the above assumes that the filaments are drawn in such a manner that they cross exactly once, if at all. If two filaments have more than one transverse intersection, add up all intersection numbers between α and β . This more general description is consistent with the above definition.

Consider any pair in \mathcal{P} , and suppose that α is a filament associated with that pair.

Definition 4.7. The *intersection number of the filament* α is

$$\langle \alpha \rangle = \sum_{\gamma \notin \{\alpha, \alpha'\}} \alpha \overline{\cap} \gamma$$

If x and y are distinct, and α and its dual α' are bifilaments associated with (x, y) , then the *intersection number of the bifilament pair* is

$$\langle (x, y) \rangle = \langle \alpha \rangle + \langle \alpha' \rangle = \sum_{\gamma \notin \{\alpha, \alpha'\}} \alpha \overline{\cap} \gamma + \alpha' \overline{\cap} \gamma.$$

Similarly, if α is the monofilament associated with the pair (x, x) , then the *intersection number of the monofilament pair* is

$$\langle (x, x) \rangle = \langle \alpha \rangle = \sum_{\gamma \notin \{\alpha, \alpha'\}} \alpha \overline{\cap} \gamma$$

Note that this can be expressed as a single formula:

Definition 4.8. The *intersection number of a pair* (x, y) , is

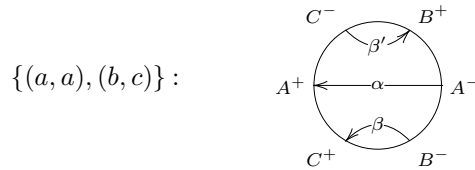
$$\langle (x, y) \rangle = \sum_{\beta \in \{\alpha, \alpha'\}} \sum_{\gamma \notin \{\alpha, \alpha'\}} \beta \overline{\cap} \gamma$$

where α is a filament associated with (x, y) .

We may need to consider multiple pairings at the same time. If this is the case, we will use a subscript $\langle \rangle_{\mathcal{P}}$ to specify which pairing we are using to calculate the intersection numbers.

Definition 4.9. A *filamentation* \mathcal{F} on a Chord Diagram \mathcal{D} , is a pairing for which the related filaments contain only transverse intersections, and the intersection number of each pair is zero.

For example, the OCD in Figure 2 has a filamentation:



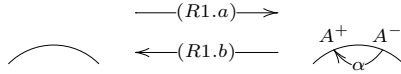
Now, we proceed with the first result.

Theorem 4.10. *If \mathcal{D} is a chord diagram which admits a filamentation \mathcal{F} , then for any chord diagram \mathcal{D}' equivalent (by Reidemeister moves) to \mathcal{D} , there is an induced filamentation \mathcal{F}' on \mathcal{D}' . Thus, the existence of a filamentation is an invariant of chord diagrams.*

Proof. Suppose \mathcal{D} is an chord diagram and \mathcal{D}' is equivalent to \mathcal{D} . Then there is a finite sequence of chord diagrams $\{\mathcal{D} = \mathcal{D}_0, \mathcal{D}_1, \dots, \mathcal{D}_n = \mathcal{D}'\}$, such that \mathcal{D}_{i+1} and \mathcal{D}_i differ by a single chord move. All we need to show is that under any of the chord moves, a filamentation can always be preserved. This will give us a filamentation \mathcal{F}_i on \mathcal{D}_i induced by each move in the sequence.

In each of the following cases, we will describe how to use the existing filamentation \mathcal{F} to create the induced filamentation \mathcal{F}' which results from applying a Reidemeister move:

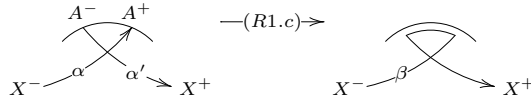
(R1) We first consider the simplest Type I cases.



If we are adding a chord, as in (R1.a), then the induced filamentation comes from taking the old filamentation and adding the pair (a, a) . We define $\mathcal{F}' = \mathcal{F} \cup \{(a, a)\}$. This gives us a monofilament α associated with the pair (a, a) . It is clear that $\langle \alpha \rangle = \langle (a, a) \rangle = 0$ since there are no chord endpoints on the circular arc between A^+ and A^- . Thus, all intersection numbers in the new filamentation are still zero.

If we remove a self-paired chord as in (R1.b), we again note that the monofilament α associated with (a, a) intersects trivially with all other filaments associated with \mathcal{F} . Thus we define $\mathcal{F}' = \mathcal{F} - \{(a, a)\}$, and it is clear that we still have a filamentation.

Finally, suppose that the chord a that is removed via a type I move is paired with another chord, say x .



In the case of (R1.c), the induced filamentation comes from altering the previous pairing by replacing the pair (x, a) with (x, x) . That is, set $\mathcal{F}' = (\mathcal{F} - \{(x, a)\}) \cup \{(x, x)\}$. This works because we can construct a new monofilament associated with (x, x) which carries the same intersections as the old bifilaments associated with (x, a) . Consider for example, the curve starting at X^- and following the path of an old filament α to A^+ , then following along the outer circle to the adjacent endpoint A^- and finally following the path of the dual filament α' to X^+ . If we adjust this curve slightly so that the circular portions of the path are pushed to within

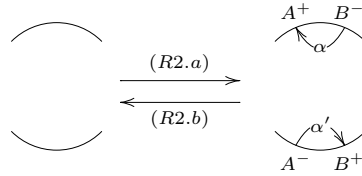
the interior of the circle (as in the above picture), we get a monofilament β associated with (x, x) . The new curve β contains the old intersections from both α and α' .

Clearly, β intersects the other filaments of \mathcal{F}' only where they coincide with the previous filaments α and α' . In addition, any old self-intersections between α and α' will be picked up, but we recall that intersections between dual filaments as well as any self-intersections do not contribute to intersection numbers. Thus, the intersection number of the new pair is

$$\langle (x, x) \rangle_{\mathcal{F}'} = \langle \beta \rangle = \langle \alpha \rangle + \langle \alpha' \rangle = \langle (x, a) \rangle_{\mathcal{F}} = 0.$$

Since all the intersections from \mathcal{F} are preserved under the new pairing, and no new intersections are introduced, \mathcal{F}' is still a filamentation.

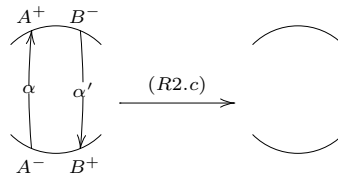
(R2) We now consider the Type II moves, starting with the simplest cases.



Whenever we add chords via a Type II move as in (R2.a), the induced filamentation comes from adding a bifilament pair (a, b) of the newly created chords. We set $\mathcal{F}' = \mathcal{F} \cup \{(a, b)\}$. The precise configuration of the chord endpoints does not affect the resulting filamentation, because in every Type II chord move, an endpoint of one chord must be adjacent to the endpoint of opposing sign from the other chord. This forces the two filaments associated with (a, b) to be curves between neighboring chord endpoints along the circle. Just as in (R1.a), each new filament will trivially intersect all other filaments in \mathcal{F}' . No other intersections are altered from the old pairing, so \mathcal{F}' is a filamentation.

Similarly, when a type II move removes a bifilament pair, as in (R2.b), the induced filamentation is $\mathcal{F}' = \mathcal{F} - \{(a, b)\}$.

The remaining cases for type II chord removal cover the other possible ways that the removed chords a and b can be paired.



Suppose a and b are self-paired as in (R2.c). Note that the possible configurations of a type II move forces the filaments to be oriented in opposing

directions, as in the picture above. As a result, for any bifilaments α and α' associated with (a,a) we have:

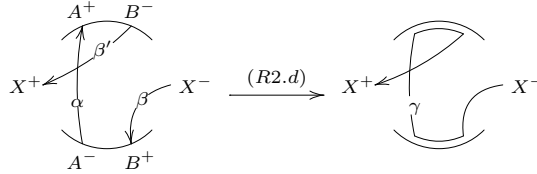
$$\langle \alpha \rangle = -\langle \alpha' \rangle$$

This also means that the net effect of α and α' on any other filament in \mathcal{F} cancels when computing the intersection number. That is, for any filament $\gamma \neq \alpha, \alpha'$, we have:

$$\begin{aligned} \langle \gamma \rangle &= \sum_{\delta \notin \{\gamma, \gamma'\}} \gamma \vec{\Pi} \delta \\ &= \left(\sum_{\delta \notin \{\gamma, \gamma', \alpha, \alpha'\}} \gamma \vec{\Pi} \delta \right) + \gamma \vec{\Pi} \alpha + \gamma \vec{\Pi} \alpha' \\ &= \sum_{\delta \notin \{\gamma, \gamma', \alpha, \alpha'\}} \gamma \vec{\Pi} \delta \end{aligned}$$

Thus, the induced filamentation for (R2.c) is $\mathcal{F}' = \mathcal{F} - \{(a, a), (b, b)\}$.

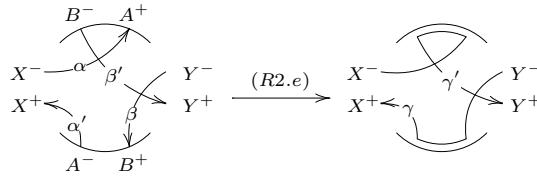
Now, suppose that either a or b are paired with a third chord, x . Without loss of generality we assume a is self-paired and b is paired with x .



In (R2.d), the induced filamentation is $\mathcal{F}' = (\mathcal{F} - \{(a, a), (b, x)\}) \cup \{(x, x)\}$. As before in (R1.c), the filament associated with the new pair (x, x) can be defined to be a curve which follows the old filaments and arcs between chord endpoints so that the locations of all intersections are preserved under the change to \mathcal{F}' . The new monofilament γ can start at X^- and follow the old paths β to α to β' (as in the picture above). To calculate the intersection number of the new filament, we simply add the intersection numbers of the filaments associated with the old pairs:

$$\begin{aligned} \langle (x, x) \rangle_{\mathcal{F}'} &= \langle \gamma \rangle \\ &= \langle \alpha \rangle + \langle \beta \rangle + \langle \beta' \rangle \\ &= \langle (a, a) \rangle_{\mathcal{F}} + \langle (b, x) \rangle_{\mathcal{F}} \\ &= 0. \end{aligned}$$

Finally, suppose a and b are both paired with other chords.



For (R2.e), we define $\mathcal{F}' = (\mathcal{F} - \{(a, x), (b, y)\}) \cup \{(x, y)\}$. Then, we define the bifilaments associated with (x, y) so that γ travels from Y^- to X^+ along β and α' , and the dual γ' travels from X^- to Y^+ along α and β' . Thus,

$$\begin{aligned}
\langle (x, y) \rangle_{\mathcal{F}'} &= \langle \gamma \rangle_{\mathcal{F}'} + \langle \gamma' \rangle_{\mathcal{F}'} \\
&= (\langle \beta \rangle_{\mathcal{F}} + \langle \alpha' \rangle_{\mathcal{F}}) + (\langle \alpha \rangle_{\mathcal{F}} + \langle \beta' \rangle_{\mathcal{F}}) \\
&= (\langle \alpha \rangle_{\mathcal{F}} + \langle \alpha' \rangle_{\mathcal{F}}) + (\langle \beta \rangle_{\mathcal{F}} + \langle \beta' \rangle_{\mathcal{F}}) \\
&= \langle (a, x) \rangle_{\mathcal{F}} + \langle (b, y) \rangle_{\mathcal{F}} \\
&= 0
\end{aligned}$$

- (R3) Suppose we have a Type III move taking \mathcal{D} to \mathcal{D}' . For any possible configuration of such a move, we define the induced filamentation to be unchanged: $\mathcal{F}' = \mathcal{F}$.

There is essentially only one AD_3 move to consider from Figure 4. This is due to the fact that the diagrams in both versions of AD_3 in Figure 4 share the same underlying OCD. As a result, the code associated with each move is the same (as are all of the local orientations on each arrow endpoint)⁶. Further, we do not need to consider each possible arc permutation as described in the discussion of Figure 4 in Section 2. As we shall see, this is because we can position the new filaments in such a way that they only differ from the previous ones within a small neighborhood of each arc involved in the move. Hence, the intersection numbers in the new filamentation will depend only on the local filament changes near these arcs.

To do this, position the filaments on \mathcal{D} so that none of the intersections occur within a small neighborhood of the circle. On the new diagram \mathcal{D}' , configure the filaments as before except within that neighborhood. Inside this neighborhood, complete the filament curves by crossing the two filaments which emanate from each arc. Note that since the AD_3 move switches the chord endpoints on each arc, these new filament crossings account for this. We show a simple example in Figure 6. On the left, the filaments leaving each arc don't cross until they pass outside a neighborhood (depicted by the dotted interior circle) of the arcs. On the right, the filaments cross as they emanate from each arc to the dotted circle. Within the interior circle, the filament curves on both diagrams are essentially the same.

Now, we consider the effect of adding this configuration of three filament crossings to the original filamentation. The general case is shown in 7. First, suppose that the chords a , b , and c are paired with other chords, x , y , and z respectively. The new crossings contribute as follows:

⁶This should not come as a surprise to the reader since a filamentation only depends on the underlying OCD's code, which means that it can be thought of as being associated with the universe of the related knot diagram.

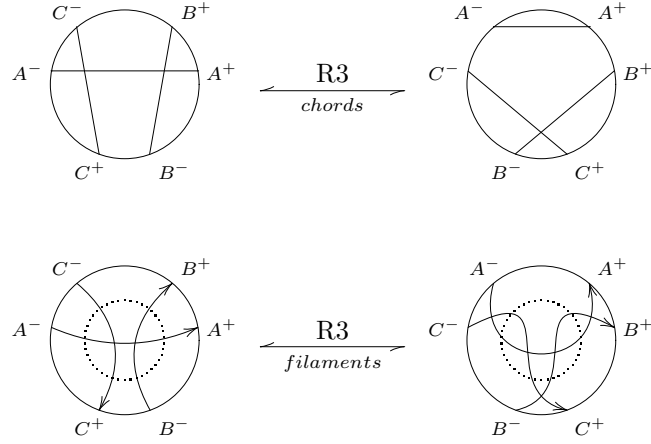


Figure 6: An example of induced filament changes under an R3 chord move

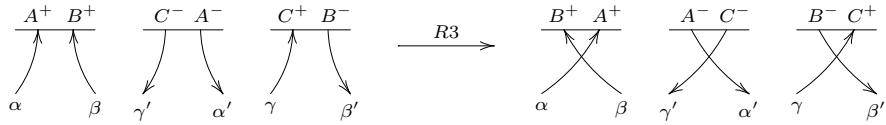


Figure 7: The general case of filament changes after an R3 chord move

$$\begin{aligned}
\langle (a, x) \rangle_{\mathcal{F}'} &= \langle (a, x) \rangle_{\mathcal{F}} + \alpha \overrightarrow{\cap} \beta + \alpha' \overrightarrow{\cap} \gamma' \\
&= 0 + 1 - 1 = 0 \\
\langle (b, y) \rangle_{\mathcal{F}'} &= \langle (b, y) \rangle_{\mathcal{F}} + \beta \overrightarrow{\cap} \alpha + \beta' \overrightarrow{\cap} \gamma \\
&= 0 - 1 + 1 = 0 \\
\langle (c, z) \rangle_{\mathcal{F}'} &= \langle (c, z) \rangle_{\mathcal{F}} + \gamma \overrightarrow{\cap} \beta' + \gamma' \overrightarrow{\cap} \alpha \\
&= 0 - 1 + 1 = 0
\end{aligned}$$

The new pairing is a filamentation whenever the old pairing is.

In fact, it does not matter how the chords are paired. For example, suppose we pair a with b . Then $x = b$, $y = a$, and from the above case, the filaments consolidate to $\alpha = \beta'$ and $\alpha' = \beta$. To compute $\langle (a, b) \rangle_{\mathcal{F}'}$, we combine the calculations of $\langle (a, x) \rangle_{\mathcal{F}'}$ and $\langle (b, y) \rangle_{\mathcal{F}'}$ above. First note

$$\langle (a, x) \rangle_{\mathcal{F}} = \langle (b, y) \rangle_{\mathcal{F}} = 0$$

Although $\alpha \overrightarrow{\cap} \alpha'$ and $\alpha' \overrightarrow{\cap} \alpha$ do not contribute to $\langle (a, b) \rangle_{\mathcal{F}'}$, they do sum to zero, so we will include them below to demonstrate the similarity to $\langle (a, x) \rangle_{\mathcal{F}'} + \langle (b, y) \rangle_{\mathcal{F}'}$:

$$\begin{aligned}
\langle (a, b) \rangle_{\mathcal{F}'} &= \langle (a, b) \rangle_{\mathcal{F}} + \alpha \overrightarrow{\cap} \alpha' + \alpha' \overrightarrow{\cap} \gamma' + \alpha' \overrightarrow{\cap} \alpha + \alpha \overrightarrow{\cap} \gamma \\
&= 0 + \alpha' \overrightarrow{\cap} \gamma' + \alpha \overrightarrow{\cap} \gamma \\
&= -1 + 1 \\
&= 0
\end{aligned}$$

Proceed in the same fashion for all other pair choices.

This completes the proof. ■

Theorem 4.11. *If \mathcal{D} is a Gauss diagram which does not admit a filamentation, then the flat knot represented by \mathcal{D} is non-trivial.*

Proof. Suppose \mathcal{D} is trivial. Then there is a sequence of flat moves taking \mathcal{D} to the unknot. Since the unknot admits a trivial filamentation, Theorem 4.10 tells us that we can find a filamentation on \mathcal{D} by reversing the sequence of flat moves and applying the filamentation induced by that sequence. Thus, if a Gauss diagram does not admit a filamentation, it cannot represent a trivial knot. ■

5 An Infinite Family of Virtual Knots

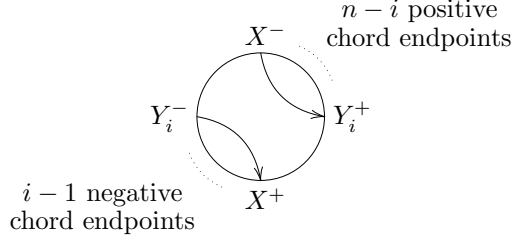
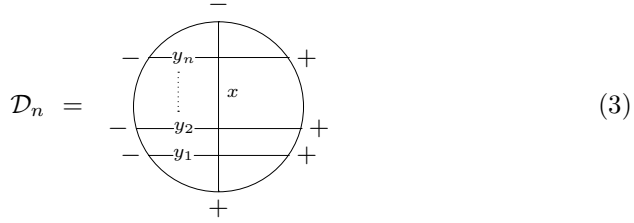


Figure 8: A biflament associated with the pair (x, y_i) in D_n .

Theorem 5.1. For $n \geq 2$, consider the following OCD:



Any flat virtual knot associated with \mathcal{D}_n is non-trivial.

Proof. Fix $n \geq 2$. Label the vertical chord x , and label the horizontal chords $\{y_1, \dots, y_n\}$. Consider the vertical chord, x . We claim that for any pairing on \mathcal{D}_n , the pair including x will always have a non-trivial intersection number.

First suppose x is self-paired. We see immediately that $\langle (x, x) \rangle = n \neq 0$, since all of the other filaments in such a pairing must pass from left to right across the monofilament associated with (x, x) .

Suppose x is paired with any of the horizontal chords, say y_i . Consider Figure 8. There are exactly $n - i$ positive chord endpoints on the arc between Y_i^+ and X^- . Regardless of how we choose to pair the remaining chords, these positive endpoints will have filaments ending at them. Further, such filaments must come from the other side of the $X^- \rightarrow Y_i^+$ filament, contributing precisely $n - 1$ to the intersection number of (x, y_i) . In addition, there are exactly $i - 1$ negative chord endpoints on the arc between Y_i^- and X^+ . Again, there must be a filament emanating from each of these negative endpoints, and each resulting filament must cross the $Y_i^- \rightarrow X^+$ filament. This adds $i - 1$ to the intersection number of (x, y_i) . Since we have covered all of the intersection numbers which contribute to the bifilaments associated with (x, y_i) , we get:

$$\langle (x, y_i) \rangle = (n - i) + (i - 1) = n - 1 > 0.$$

This means that there are no filamentations on any \mathcal{D}_n when $n \geq 2$, so by Theorem 4.11, any flat knot associated with \mathcal{D}_n must be nontrivial. \blacksquare

Theorem 5.1 gives us an infinite set of OCD's for which any flat representative must be non-trivial. We don't yet have a proof that they give rise to distinct flat knots, but we believe this to be the case.

Conjecture 5.2. *The flat knots U_n in (3) are distinct for all $n \geq 1$.*

One interesting result we have found is a related infinite class of virtual knot diagrams, depicted in Table 1. As we shall see, they are all distinct. What is even more interesting about this class is that each knot has trivial Jones polynomial and trivial fundamental group. This gives the first example of an infinite class of virtual knots with trivial Jones polynomial and trivial fundamental group.

5.1 The Jones Polynomial via the Kauffman Bracket

Many of the results stated in this section are from [13, 14]. Another nice reference containing the known properties of the (normalized) Kauffman bracket and the Jones polynomial is [16].

To compute the bracket polynomial in the case of classical knots, we start with the skein relation:

$$\left\langle \begin{array}{c} \diagup \diagdown \\ \diagdown \diagup \end{array} \right\rangle = A \left\langle \begin{array}{c} \diagup \\ \diagdown \end{array} \right\rangle \left\langle \begin{array}{c} \diagdown \\ \diagup \end{array} \right\rangle + A^{-1} \left\langle \begin{array}{c} \cup \\ \cup \end{array} \right\rangle \quad (4)$$

Using (4), expand each crossing in a knot diagram until we are left with a sum of collections of closed curves, called *states*. To evaluate the bracket on a state, we apply the following:

$$\left\langle \begin{array}{c} \bigcirc \\ K \end{array} \right\rangle = \delta \langle K \rangle = (-A^2 - A^{-2}) \langle K \rangle \quad (5)$$

$$\left\langle \begin{array}{c} \bigcirc \end{array} \right\rangle = 1 \quad (6)$$

The bracket extends naturally to the virtual category. As above, a state of a virtual knot diagram is the result of smoothing all real crossings. A closed curve in such a state might still contain virtual crossings. Ignore the virtual crossings and count the number of closed curves $\|S\|$ in the state. Assign the value of $\delta^{\|S\|-1}$ to each state. Since the bracket is a regular isotopy invariant, we need to normalize it to get an invariant of virtual knots under ambient isotopy.

Definition 5.3. Let K be a virtual knot diagram. The *writhe* of K is the sum

$$w(K) = \sum_{x \in C(K)} \epsilon(x),$$

where $C(K)$ denotes the set of all real crossings in K .

n	\mathcal{D}_n	U_n	\mathcal{A}_n	K_n
0				
1				
2				
3				
⋮	⋮	⋮	⋮	⋮

Table 1: The class of virtual knots arising from D_n .

Definition 5.4. If K is a virtual knot, then the normalized bracket is given by

$$f_K(A) = (-A^3)^{-wr(K)} \langle K \rangle$$

For example, we compute the bracket of the positive virtual Hopf link:

$$\begin{aligned} \langle VHopf_+ \rangle &= \left\langle \begin{array}{c} \text{Diagram of } VHopf_+ \text{ with a crossing} \end{array} \right\rangle \\ &= A \left\langle \begin{array}{c} \text{Diagram of } VHopf_+ \text{ with a crossing} \end{array} \right\rangle + A^{-1} \left\langle \begin{array}{c} \text{Diagram of } VHopf_+ \text{ with a crossing} \end{array} \right\rangle \\ &= A + A^{-1} \end{aligned}$$

and the normalized bracket is then

$$f_{VHopf_+}(A) = (-A^3)^{-(+1)} \langle VHopf_+ \rangle = -A^{-3}(A + A^{-1}) = -A^{-2} - A^{-4}.$$

If K is a knot diagram and K^* is the diagram obtained by switching all the crossings in K , we have the well known property $f_{K^*}(A) = f_K(A^{-1})$. This gives us the normalized bracket on the negative virtual Hopf:

$$f_{VHopf_-}(A) = f_{VHopf_+}(A^{-1}) = -A^2 - A^4$$

An immediate result is that $VHopf_+$ and $VHopf_-$ are distinct.

Another well known result is the connection between the normalized bracket and the Jones polynomial:

Theorem 5.5. Let K be a knot and $V_K(t)$ be the Jones polynomial of K . Then

$$V_K(t) = f_K(t^{-\frac{1}{4}})$$

In the case of classical knots (of one component), the Jones polynomial is always an element of $\mathbb{R}[t, t^{-1}]$, and hence the normalized bracket gives rise to polynomials in $\mathbb{R}[A^4, A^{-4}]$. However, when generalized to include virtual knots, the Jones and normalized bracket polynomials on single component virtual knots turn out to be in $\mathbb{R}[t^{\frac{1}{2}}, t^{-\frac{1}{2}}]$ and $\mathbb{R}[A^2, A^{-2}]$ respectively. This means that some virtual knots can be detected by looking for non-integral powers of t in the evaluation of the Jones polynomial (or odd powers of A^2 in the normalized bracket).

5.2 Virtual Knots Related to \mathcal{A}_n Have Trivial Jones Polynomial

Theorem 5.6 (Kauffman [13]). *The bracket is invariant under the following moves*

$$\begin{aligned} \langle \text{Diagram 1} \rangle &= \langle \text{Diagram 2} \rangle \\ \langle \text{Diagram 3} \rangle &= \langle \text{Diagram 4} \rangle \end{aligned} \quad (7)$$

Translating the above to arrow diagrams, we have:

$$\langle \left(\begin{array}{c} \epsilon \\ \longrightarrow \\ \epsilon \end{array} \right) \rangle = \langle \left(\begin{array}{c} \longleftarrow \\ \epsilon \end{array} \right) \rangle \quad (8)$$

Equation (8) implies that other than the general configuration of the chords, the bracket depends only on the local orientations of the arrow basepoints in an arrow diagram. The direction of an arrow can change, provided that the local orientations of the endpoints change with it. Thus the relevant signs stay the same, as does the writhe. This brings us back to what we stated in Section 2. The normalized bracket (and hence the Jones polynomial) is an invariant of signed chord diagrams. This will be the subject of another paper.

Definition 5.7. If V and V' are two virtual knots for which $f_V(A) = f_{V'}(A)$, then V and V' are said to be *Jones equivalent*. The same expression can refer to chord diagrams.

There are many examples of virtual knots which are Jones equivalent. Consider the AD_2 move. Changing one arrow direction results in

$$\langle \left(\begin{array}{c} \longleftarrow \\ \epsilon \quad -\epsilon \\ \longrightarrow \end{array} \right) \rangle = \langle \left(\begin{array}{c} \longleftarrow \\ \quad \\ \end{array} \right) \rangle = \langle \left(\begin{array}{c} \epsilon \\ \longrightarrow \\ -\epsilon \end{array} \right) \rangle \quad (9)$$

It is easy to construct infinite families of Jones equivalent virtual knots. Take any arrow diagram \mathcal{A} . Then choose two empty arcs within it, and apply (9) an arbitrary number of times. The K_n in Table 1 are an example of this.

Theorem 5.8. *If K_n is a virtual knot associated with \mathcal{A}_n , then $f_{K_n}(A) = 1$.*

Proof. The first two AD's, \mathcal{A}_0 and \mathcal{A}_1 are representatives of the trivial knot class. \mathcal{A}_0 is a direct result of applying AD_1 to the unknot diagram, and \mathcal{A}_1 is the result of applying AD_2 to the unknot diagram. The rest of the \mathcal{A}_n are also Jones equivalent to the unknot, because

- for even n , the \mathcal{A}_n are Jones equivalent to \mathcal{A}_0 , and
- for odd n , the \mathcal{A}_n are Jones equivalent to \mathcal{A}_1 .

This is because each \mathcal{A}_n in Table 1 is Jones equivalent to \mathcal{A}_{n+2} by a single application of (9) on the horizontal arrows. As a result, each K_n is Jones equivalent to the unknot and hence the normalized bracket will be trivial on all of them. ■

We should point out that Jones equivalence does not necessarily come only from transformations of the form in (7) and (8). There are also classical knots such as mutants, for example, which are Jones equivalent to each other. We doubt that mutants can be obtained through (7) alone.

A well known open question is the following: are there non-trivial classical knots which are Jones equivalent to the unknot? In other words, does the Jones polynomial detect knottedness for classical knots?

Conjecture 5.9. *If K is a non-trivial classical knot, then $f_K(A) \neq 1$.*

5.3 The Fundamental Group and the Quandle

Definition 5.10. A *quandle* [13] Q is a non-associative algebraic system with two binary operations represented through the symbols $\overline{\quad}$ and $\underline{\quad}$ which satisfy the following axioms:

1. For every $a \in Q$, $a\overline{a} = a$ and $a\underline{a} = a$.
2. For every $a, b \in Q$, $a\overline{b\overline{b}} = a$ and $a\underline{b\underline{b}} = a$.
3. For every $a, b \in Q$, there is an $x \in Q$ such that $x = a\overline{b}$ and $a = x\overline{b}$.
The left/right variant of this statement must also be true:
For every $a, b \in Q$, there is an $x \in Q$ such that $x = a\underline{b}$ and $a = x\underline{b}$.
4. For every $a, b, c \in Q$, the following two equations hold, along with their left/right variants:

$$\begin{aligned} a\overline{b}\overline{c} &= a\overline{c}\overline{b\overline{c}} \\ a\underline{b}\underline{c} &= a\underline{c}\underline{b\underline{c}} \end{aligned}$$

See [15] for more on the formalism of the operator notation $\overline{\quad}$ and $\underline{\quad}$. The notation is useful because it allows us to write expressions in a non-associative setting without requiring lots of parentheses. The operators assume a left associative convention, and when an expression is associated differently, the over and under bars serve as parentheses by extending over or under the entire sub-expression acted upon.

For example, we can think of $\overline{\quad}$ as the binary operator $*$, and $\underline{\quad}$ as $\bar{*}$. Then $a * b = a\overline{b}$, $a \bar{*} b = a\underline{b}$, and the two basic associations are:

$$\begin{aligned} (a * b) * c &= a\overline{b}\overline{c} \\ a * (b * c) &= a\overline{b\overline{c}} \end{aligned}$$

Use the same convention for both operators. Here are some mixed expressions:

$$\begin{aligned} (a \bar{*} b) * b &= a\overline{b\overline{b}} \\ a * (b \bar{*} (c * d)) &= a\overline{b\overline{c\overline{d}}} \end{aligned}$$

The axioms of a quandle make it possible to associate quandles with knots and links in such a way that the algebraic structure is invariant under the Reidemeister moves.

A *bridge arc* in a virtual diagram is a strand between the undercrossings of two (possibly the same) classical crossings. In the same sense, an *arc* in a diagram is a strand directly between any two classical crossings. This means that a bridge arc is interpreted on an arrow diagram as an arc directly between terminating endpoints of arrows. An arc is a portion of the circle directly between any two arrow endpoints. For example, there are two arcs in V_0 and the related arrow diagram \mathcal{A}_0 , whereas there is only one bridge arc.

We define a quandle $Q(K)$ associated with a knot K as follows. Start with an oriented diagram. Assign one generator to each bridge arc. For each classical crossing, depending on crossing orientation, assign an equivalence according to the following rule:

$$\begin{array}{ccc}
 \begin{array}{c} c = b \overline{a} \\ \swarrow \quad \nearrow \\ a \quad b \end{array} & & \begin{array}{c} b \quad c = a \overline{b} \\ \swarrow \quad \nearrow \\ a \quad b \end{array} \\
 & & (10)
 \end{array}$$

We say a quandle rather than the quandle, because we refer to any quandle satisfying these properties. There is a universal construction [11] for a quandle associated with a knot, but we will not discuss that construction here.

Setting $b \overline{a} = bab^{-1}$ and $a \overline{b} = a^{-1}ba$ in the universal construction gives the fundamental group of the complement of a classical knot. We will denote $\pi_1(K)$ to be the fundamental group of a virtual knot K obtained via the quandle.

5.4 Virtual Knots Related to \mathcal{A}_n Have Trivial Quandles

Lemma 5.11. *If we evaluate the quandle on*



where the box is replaced by a sum of the following elementary 4-tangles



then $a = b = c$. The tangle introduces no further equations.

Proof. We leave this proof as an exercise. ■

Theorem 5.12. *If K_n is a virtual knot associated with \mathcal{A}_n , then $\pi_1(K_n) = 0$.*

Proof. In the right column of Table 1, we have representative virtual knots K_n for each \mathcal{A}_n . By Theorem 3.4, if we prove $\pi_1 = 0$ on each of these, we are done. We will prove this via the quandle. First note that each K_n in Table 1 are of the general form:



where the box is replaced by a horizontal sum of elementary 4-tangles.

In (11), we have labeled the bridge arc emanating from the lower left side of the tangle by the generator a . Note that this bridge arc both enters and exits the left side of the tangle. Both strands entering the left of the box are labeled with the generator a . By 5.11, we see that the strands emanating from the right of the box can also be labeled a . As a result, every bridge arc in the knot diagram can be labeled with the same generator, and the quandle is trivial. ■

6 The Alexander Biquandle

In the construction of a quandle, we can think of each crossing as an input/output diagram with the labels on the strands that go into the crossing as inputs to a function, and labels on the strands that go out of the crossing as outputs of that function. This idea leads to the biquandle [6, 15, 9]. With the quandle, the overcrossing strand carries a label unchanged across the diagram, while the undercrossing strand changes its label in a manner which depends on both input labels.

In a biquandle, the overcrossing strand may also change its label. This requires the definition of four separate functions for the output strand labels, as illustrated in Figure 9. We indicate these functions by the symbolism

$$a \overline{b} \quad a \underline{b} \quad a \overline{\overline{b}} \quad a \overline{\underline{b}}$$

and view both the inputs and outputs from left to right. Note that each of the symbols $\overline{\quad}$, $\underline{\quad}$, $\overline{\overline{\quad}}$ and $\overline{\underline{\quad}}$, can be regarded as a binary operation on the underlying set of the biquandle. Using this symbolism, the functions for the left and right crossings are

$$R \begin{bmatrix} a \\ b \end{bmatrix} = \begin{bmatrix} \overline{b \overline{a}} \\ a \underline{b} \end{bmatrix} \quad L \begin{bmatrix} a \\ b \end{bmatrix} = \begin{bmatrix} \overline{b \underline{a}} \\ a \overline{\overline{b}} \end{bmatrix}$$

In order for these functions to define a biquandle, they must exhibit invariance under the Reidemeister moves. We omit the details here.

The Alexander biquandle is an example of a biquandle, and we will only deal with its specific properties.

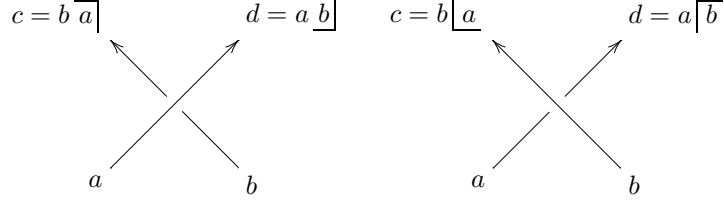


Figure 9: The Biquandle Operations

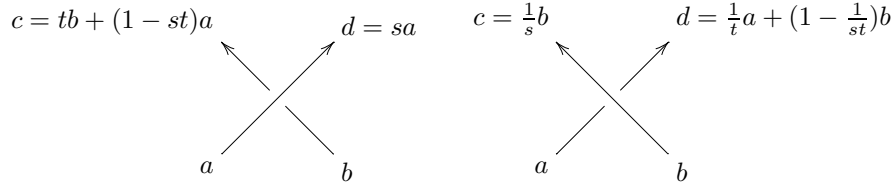


Figure 10: The Alexander Biquandle Operations

Consider any module M over the ring $R = \mathbb{Z}[s, s^{-1}, t, t^{-1}]$. Defining the binary operations with the following equations provides us with a biquandle structure on M :

$$a \overline{b} = ta + (1 - st)b \quad a \underline{b} = sa \quad (12)$$

$$a \overline{b} = \frac{1}{t}a + (1 - \frac{1}{st})b \quad a \underline{b} = \frac{1}{s}a \quad (13)$$

If M is a free module, we call this a *free Alexander biquandle*.

We associate a specific biquandle to a virtual knot diagram by taking the free module obtained by assigning one generator for each arc and factoring out by the submodule generated by the relations given in (12). We call the resulting module $ABQ(K)$ the *Alexander biquandle of the knot K* .

Note that

$$R \begin{bmatrix} a \\ b \end{bmatrix} = \begin{bmatrix} b \overline{a} \\ a \underline{b} \end{bmatrix} \quad (14)$$

$$= \begin{bmatrix} tb + (1 - st)a \\ sa \end{bmatrix} \quad (15)$$

$$= \begin{pmatrix} 1 - st & t \\ s & 0 \end{pmatrix} \begin{bmatrix} a \\ b \end{bmatrix} \quad (16)$$

is a linear map, and R can be represented by the matrix A given in Table 2. Similarly, the function L can be represented by the matrix B in the Table.

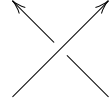
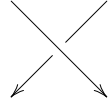
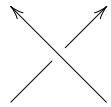
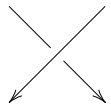
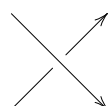
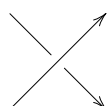
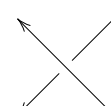
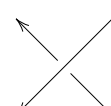
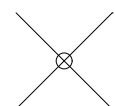
	: $A = \begin{pmatrix} 1-st & t \\ s & 0 \end{pmatrix}$		: $\hat{A} = \begin{pmatrix} 0 & s \\ t & 1-st \end{pmatrix}$
	: $B = \begin{pmatrix} 0 & \frac{1}{s} \\ \frac{1}{t} & 1-\frac{1}{st} \end{pmatrix}$		: $\hat{B} = \begin{pmatrix} 1-\frac{1}{st} & \frac{1}{t} \\ \frac{1}{s} & 0 \end{pmatrix}$
	: $C = \begin{pmatrix} 0 & \frac{1}{s} \\ t & \frac{1}{s}-t \end{pmatrix}$		: $\hat{C} = \begin{pmatrix} \frac{1}{s}-t & t \\ \frac{1}{s} & 0 \end{pmatrix}$
	: $D = \begin{pmatrix} 0 & s \\ \frac{1}{t} & s-\frac{1}{t} \end{pmatrix}$		: $\hat{D} = \begin{pmatrix} s-\frac{1}{t} & \frac{1}{t} \\ s & 0 \end{pmatrix}$
			
: $V = \begin{pmatrix} 0 & 1 \\ 1 & 0 \end{pmatrix}$			

Table 2: Matrices for the Alexander biquandle

Since we are dealing with linear functions, we need not restrict our inputs and outputs according to the direction of the strands. Instead, we can choose any two adjacent strands as inputs, and compute the resulting function by inverting or changing the basis of the original matrices A and B . To maintain a input/output convention which is consistent with before, we will order inputs in a counter-clockwise direction and outputs in a clockwise direction.

Note that we have inserted a matrix V in Table 2, which permutes the inputs. This matrix represents the virtual crossing, where labels are passed along the strands without any changes.

The set of relations for a presentation of $ABQ(K)$ contains a generalization of the Alexander polynomial (see [10, 15, 20, 21]).

Definition 6.1. The *Generalized Alexander Polynomial* of K , $G_K(s, t)$ is the determinant of the relation matrix from a presentation of $ABQ(K)$. Up to multiples of $\pm s^i t^j$ for $i, j \in \mathbb{Z}$, it is an invariant of K .

This polynomial is a zeroth order polynomial. It vanishes on classical knots

and links.

Recall that in the previous section, the flat knots U_n are non-trivial. The generalized Alexander polynomial provides us with the tools to show that the related collection of knots K_n are all distinct.

Theorem 6.2. *The virtual knots K_n are all distinct for $n > 0$.*

Proof. We use the following model as our general form for the K_n :

$$K_n = \text{Diagram} \quad (17)$$

The arrows show the direction we will use for the matrix insertions. The simplified relations are:

$$X_n \cdot \begin{bmatrix} b \\ c \end{bmatrix} = \begin{bmatrix} a \\ d \end{bmatrix} \quad Y \cdot \begin{bmatrix} b \\ a \end{bmatrix} = \begin{bmatrix} c \\ d \end{bmatrix} \quad (18)$$

Using the matrices from Table 2 to calculate the Generalized Alexander polynomial on K_n , we have

$$Y = AV = \begin{pmatrix} t & 1 - st \\ 0 & s \end{pmatrix}$$

Now set $X = \begin{pmatrix} x_{11} & x_{12} \\ x_{21} & x_{22} \end{pmatrix}$, so that $G_{K_n}(s, t)$ is the following determinant:

$$G_{K_n}(s, t) = \begin{vmatrix} 1 - st & t & -1 & 0 \\ s & 0 & 0 & -1 \\ -1 & x_{11} & x_{12} & 0 \\ 0 & x_{21} & x_{22} & -1 \end{vmatrix}$$

The general form for X_n depends on whether n is odd or even.

$$X_n = \begin{cases} V(CV\widehat{C}V)^k = V(C^2)^k = VC^n, & \text{if } n = 2k, k \geq 0; \\ V\widehat{D}V(CV\widehat{C}V)^k = C(C^2)^k = C^n, & \text{if } n = 2k + 1, k \geq 0. \end{cases} \quad (19)$$

With a little help from Maple,

$$C^n = \begin{pmatrix} \frac{(-t)^n + ts^{(1-n)}}{st+1} & \frac{-(-t)^n + s^{-n}}{st+1} \\ \frac{t(-s(-t)^n + s^{(1-n)})}{st+1} & \frac{ts(-t)^n + s^{-n}}{st+1} \end{pmatrix} \quad (20)$$

For n even

$$\begin{aligned}
G_{K_n}(s, t) &= \begin{vmatrix} 1-st & t & -1 & 0 \\ s & 0 & 0 & -1 \\ -1 & \frac{t(-s(-t)^n+s^{(1-n)})}{st+1} & \frac{ts(-t)^n+s^{-n}}{st+1} & 0 \\ 0 & \frac{(-t)^n+ts^{(1-n)}}{st+1} & \frac{-(-t)^n+s^{-n}}{st+1} & -1 \end{vmatrix} \\
&= \frac{s^n(s^2t+1)(1-t) + s^2t^2 - 1 + (1-s^2)t^{(1-n)}}{st+1}
\end{aligned}$$

and for n odd,

$$\begin{aligned}
G_{K_n}(s, t) &= \begin{vmatrix} 1-st & t & -1 & 0 \\ s & 0 & 0 & -1 \\ -1 & \frac{(-t)^n+ts^{(1-n)}}{st+1} & \frac{-(-t)^n+s^{-n}}{st+1} & 0 \\ 0 & \frac{t(-s(-t)^n+s^{(1-n)})}{st+1} & \frac{ts(-t)^n+s^{-n}}{st+1} & -1 \end{vmatrix} \\
&= \frac{s^{(n+1)}(1-t^2) + s^2t^2 - 1 + (1-s^2)t^{(1-n)}}{st+1}
\end{aligned}$$

The polynomials $s^n(s^2t+1)(1-t)$ and $s^{(n+1)}(1-t^2)$ are distinct for any $n \geq 0$. This proves the theorem. \blacksquare

7 Open Problems

There are many unanswered questions in flat virtual knot theory. In addition to the difficulty of determining when a flat knot is trivial, it is also hard to distinguish between two flat virtual knots. In this paper, we have given methods to determine the non-triviality of some flat virtual knots. We have investigated the family U_n of flat virtual knots that are shadows of the knots K_n . We showed in this paper that each K_n is distinct from the others. It is conjectured that the U_n are all distinct as flat virtual knots.

An intriguing example of a flat knot conjectured to be non-trivial is the flat Kishino knot, shown in Figure 11. This diagram is not detected by filamentation techniques, nor any other approach that we know. In addition, the Kishino virtual knot shown in the same figure is undetectable by biquandles and the Jones polynomial. It has been shown to be detected by the 3-stranded Jones polynomial [17].

We do have a simple biquandle invariant that can detect flat links. It is a specialization of the Alexander Biquandle that is described by the labellings:

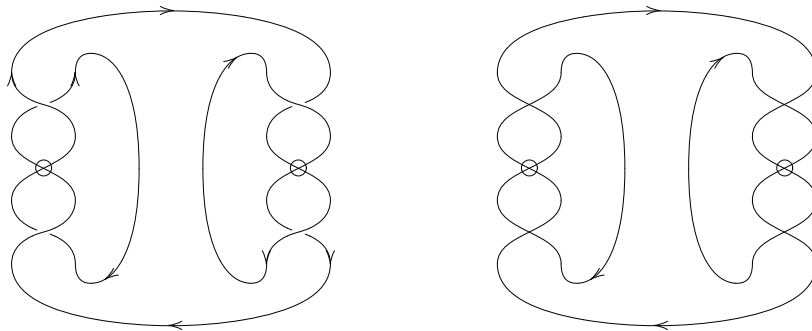
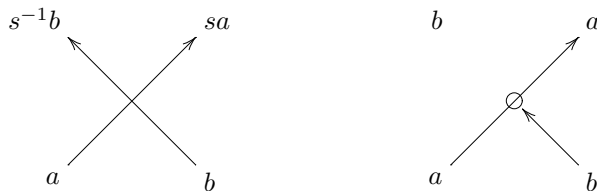


Figure 11: A non-trivial virtual knot (Kishino's example)



These labellings give a module structure associated with a flat diagram in the same way as the Alexander Biquandle. Figure 12 illustrates an example link L' whose flat biquandle is generated by elements a and b , with relations $s^2a = a$ and $s^{-2}b = b$. Since the unlink of two components has a module with generators a and b and no relations. This shows that L' is linked (where direct parity counts fail). Clearly, much more work remains to be accomplished in this field.

At this writing, it is not known how to extend the filamentation invariant to links. More generally, we would like to have more powerful combinatorial tools to distinguish flat virtual knots and links.

References

- [1] D. Bar-Natan. On the Vassiliev Knot Invariants. *Topology*, 34(2):423–472, 1995.
- [2] J. S. Carter. Classifying Immersed Curves. *Proc. Amer. Math. Soc.*, 111(1):281–287, Jan 1991.

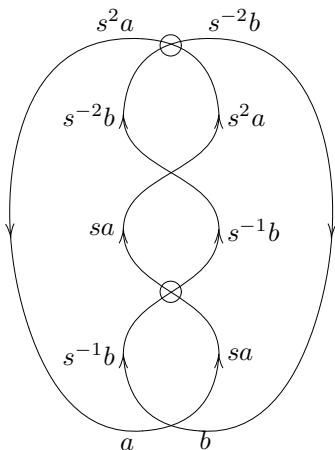


Figure 12: An example of how to compute the flat biquandle on a knot

- [3] J. S. Carter. Closed Curves that Never Extend to Proper Maps of Disks. *Proc. Amer. Math. Soc.*, 113(3):879–888, Nov 1991.
- [4] J. S. Carter. Extending Immersed Curves to Proper Immersions of Surface. *Topology and its Applications*, 40:287–306, 1991.
- [5] R. Fenn. The Braid-Permutation Group. *Topology*, 36(1):123–135, 1997.
- [6] R. Fenn, M. Jordan, and L. H. Kauffman. Biracks, Biquandles and Virtual Knots. (*preprint*), 2002.
- [7] R. Fenn, R. Rimànyi, and C. Rourke. Some Remarks on the Braid-Permutation Group. *Topics in Knot Theory*, pages 57–68, 1993.
- [8] M. Goussarov, M. Polyak, and O. Viro. Finite Type Invariants of Classical and Virtual Knots. *Topology*, 39:1045–1068, 2000.
- [9] D. Hrencecin. *On Filamentations and Virtual Knot Invariants*. PhD thesis, Univ. of Illinois at Chicago, October 2001.
- [10] F. Jaeger, L. H. Kauffman, and H. Saleur. The Conway Polynomial in \mathbb{R}^3 and in Thickened Surfaces: a New Determinant Formulation. *J. Combin. Theory*, 61:237–259, 1994.
- [11] D. Joyce. A Classifying Invariant of Knots, the Knot Quandle. *J. Pure Appl. Algebra*, 23(1):37–65, 1982.
- [12] L. H. Kauffman. *On Knots*, volume 115 of *Annals of Mathematics Studies*. Princeton University Press, 1987.

- [13] L. H. Kauffman. Virtual Knot Theory. *European J. Comb.*, 20:663–690, 1999.
- [14] L. H. Kauffman. Detecting Virtual Knots. *Atti. Sem. Mat. Fis. Univ. Modena*, 49:241–282, 2001.
- [15] L. H. Kauffman and D. E. Radford. Bi-Oriented Quantum Algebras and a Generalized Alexander Polynomial for Virtual Links. (*preprint - arXiv:math.GT/0112280*), 2001.
- [16] A. Kawauchi. *A Survey of Knot Theory*. Birkhäuser, 1996.
- [17] T. Kishino and S. Satoh. A Note on Non-Classical Virtual Knots. (*To appear in JKTR*), 2002.
- [18] M. Polyak. On the Algebra of Arrow Diagrams. *Lectures in Mathematical Physics*, 51:275–291, 2000.
- [19] M. Polyak and O. Viro. Gauss Diagram Formulas for Vassiliev Invariants. *Int. Math. Res. Notices*, 11:445–454, 1994.
- [20] J. Sawollek. On Alexander-Conway Polynomials for Virtual Knots and Links. (*preprint - arXiv:math.GT/9912173*), 1999.
- [21] D. S. Silver and S. G. Williams. Alexander Groups and Virtual Links. *JKTR*, 10:151–160, 2001.